

# Passive Optical Network for CDMA-Based Microcellular Communication Systems

H. Kim, *Associate Member, IEEE*, and Y. C. Chung, *Member, IEEE, Member, OSA*

*Invited Paper*

**Abstract**—An analog fiber-optic link transporting the wireless code-division multiple-access (CDMA) signals requires the minimum dynamic range of only about 30 dB. Motivated by this relaxed requirement, we have recently proposed a passive optical network for CDMA-based microcellular communication systems. In this paper, we reviewed the basic design rules and demonstrated various networks using double-star and ring architectures. We implemented these networks by using inexpensive light sources such as a Fabry–Perot laser (for downstream) and light-emitting diodes (for upstream). The results show that these networks could support more than eight remote base stations located within  $\sim 10$  km from the central base station.

**Index Terms**—Code division multiple access (CDMA), passive optical network (PON), personal communication service (PCS), subcarrier multiplexing (SCM), wireless communication.

## I. INTRODUCTION

**D**UE TO the explosive growth of wireless communication in recent years, network operators are having tremendous difficulties accommodating the increasing traffic. The microcellular system could relax this problem by utilizing the radio spectrum efficiently and enhancing the system's capacity. It could also reduce the power consumption of the mobile transceivers (i.e., handset), as the cell diameter becomes smaller than a few hundreds of meters. However, the reduced cell size imposes new problems: a large number of remote base stations (RBSs) should be installed within small areas and the network should be able to ensure the seamless connection among the numerous RBSs. Thus, for the practical implementation of microcellular systems, it is essential to reduce the cost and size of RBSs and move the complicate control circuitry to the central base station (CBS). Fiber-optic network offers many advantages for this purpose [1]–[7]. Fig. 1 shows a typical fiber-optic network for wireless communication system. In this network, the modulators (MOD) and demodulators (DEM) are placed at the CBS and the radio signals are transported by optical fibers using subcarriers. Thus, each RBS consists of only an electric-to-optic (E/O) converter, an optic-to-electric (O/E) converter, and electrical amplifiers. These small RBSs could be mounted on the electric poles in the street and reduce the installation costs. In addition, it would

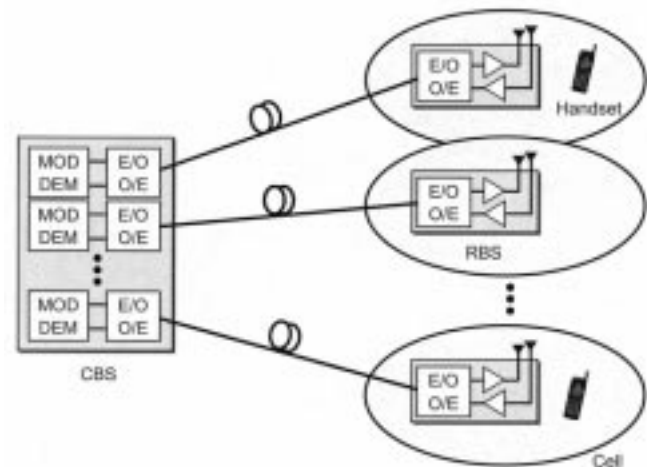


Fig. 1. Fiber-optic link for wireless communication systems.

simplify the operation and maintenance of the network since all the complicate control equipment is housed at the CBS. However, the most important advantage of this network should be attributed to the transparency of fiber-optic links. In this subcarrier-multiplexed (SCM) network, the RBS simply acts as a remote antenna. Thus, the network operators should be able to upgrade their network without changing the RBSs. For example, the modulation format of the radio signals could be changed simply by replacing the modulators and demodulators at the CBS. The dynamic channel allocation could also be achieved easily since all the channel assignment and management functions are processed at the CBS. Thus, it would be possible to provide a new type of service without changing the RBSs (as long as the electric amplifiers in RBSs have wide enough bandwidth to support these new services).

One of the most important parameters in designing the fiber-optic network for microcellular systems would be the dynamic range required for the upstream transmission from RBS to CBS. This is mainly because the upstream E/O converter must be able to handle the large variation of received signal power from different mobile transceivers. For example, even when the cell diameter is only about 1 km, the signal power received at the RBS antenna could vary as much as 80–90 dB due to the fading by multipath reflections and/or shadowing by natural or artificial objects [3]. To characterize the dynamic range requirement of fiber-optic link, it is useful to utilize the

Manuscript received April 3, 2000; revised August 17, 2000. This work was supported in part by the NRL program of MOST.

The authors are with the Department of Electrical Engineering, Korea Advanced Institute of Science Technology, Taejon 305-701, Korea.

Publisher Item Identifier S 0733-8724(01)01897-7.

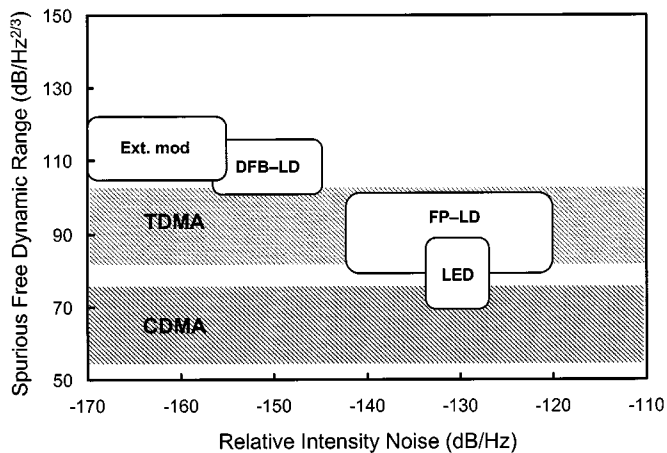


Fig. 2. Achievable SFDR for various optical transmitters. In this figure, we assumed that the received signal power could range from 0.2 to 5 mW for DFB and FP lasers. In the case of LEDs, however, the received signal power was assumed to be in the range of 10–100  $\mu$ W. We also assumed that the input third-order intercept point of the optical transmitters was 20–30 dBm. It should be noted that the SFDR requirements of both TDMA- and CDMA-based systems (shaded areas) included the system margin of 10 dB.

spurious-free dynamic range (SFDR). The SFDR is an input signal range in which the carrier-to-noise ratio (CNR) exceeds one and the two-tone third-order intermodulation product could be neglected. Thus, the SFDR represents only the performance of the fiber-optic link. In general, the SFDR is limited by the performance of the optical transmitters, since the fiber-optic link for wireless communication system typically operates over a short distance ( $< \sim 10$  km). Fig. 2 shows the achievable SFDRs for various optical transmitters. To obtain the high SFDR over 120 dB/Hz<sup>2/3</sup>, it is necessary to use a high-power optical source with low relative intensity noise (RIN), such as an Nd:YAG laser and a low-distortion external modulator [3]. The inexpensive optical sources such as Fabry–Perot (FP) lasers and light-emitting diodes (LEDs) can achieve the SFDR of only 70–100 dB/Hz<sup>2/3</sup> [7].

Recently, code-division multiple-access (CDMA) technology has been introduced for the personal communication service (PCS) systems [8]. It has been reported that the CDMA-based systems have about three times greater capacity than the systems using the time-division multiple-access (TDMA) technology.<sup>1</sup> In addition, CDMA has been selected as a standard radio transmission technology for International Mobile Telecommunication-2000 (IMT-2000). (See TIA Standards and Technologies: <http://www.tiaonline.org/standards/>.) However, the upstream performance of the CDMA-based system could be limited by the interference from other users (i.e., a strong signal from a certain user could degrade the performances of other users due to the near–far problem). Thus, the CDMA-based system employs a strong power control scheme in the mobile transceivers (on the order of 80 dB in commercial PCS systems) [9]. Due to this tight power control involved in the CDMA mobile transceivers, the required dynamic range of upstream transmission is relaxed significantly. Fig. 2 shows that the analog fiber-optic links for CDMA-based

systems would require the SFDR of only 55–75 dB/Hz<sup>2/3</sup> (including 10 dB for margin and 5 dB for spectral fluctuation of the CDMA signals) for the upstream transmission [7], [12], [13]. On the other hand, in TDMA-based systems such as Global System for Mobile Communications (GSM) and Digital Cellular System-1800 (DCS-1800), the mobile transceivers are typically designed to control the transmitted powers up to about 28 dB [9]. Accordingly, it has been reported using simulations that the fiber-optic link transporting TDMA-based signals would require the SFDR of 82–102 dB/Hz<sup>2/3</sup> including 10-dB margin, which is 20–30 dB higher than the CDMA-based systems [10], [11]. Because of this stringent dynamic range requirement of TDMA-based systems, all the previously demonstrated fiber-optic networks for wireless communication systems were based on the single-star architecture [1]–[3], [5], [6]. In addition, these networks utilized high-performance optical transmitters at the RBSs. We have recently pointed out that, unlike the TDMA-based systems, the fiber-optic networks for CDMA-based systems could have various network architectures (including double-star, bus, and ring) and utilize low-cost optical sources at RBSs since their dynamic range requirement is mitigated by more than 20 dB [12]–[16].

In this paper, we propose and demonstrate the passive optical networks (PONs) for CDMA-based microcellular communication systems. In Section II, we describe the performances of these networks based on double-star architecture. To examine the possibility of implementing the proposed network with inexpensive optical sources, we compared the network performances with DFB lasers, FP lasers, and LEDs. In Section III, we demonstrate a bidirectional PON to enhance the cost-effectiveness of the proposed network. However, these networks, based on the double-star architecture, are vulnerable to fiber failures. In Section IV, we show that the proposed network can also be implemented with ring architecture for the self-healing capability. There was no significant difference on the network's scalability between these two architectures. Finally, this paper is summarized in Section V.

## II. PASSIVE OPTICAL NETWORK FOR CDMA-BASED WIRELESS COMMUNICATION SYSTEM

Fig. 3 shows the dynamic range of upstream CDMA signals measured at the PCS base stations operating for commercial services. We measured the received powers of CDMA signals every 20 milliseconds for about 40 h by using an RF spectrum analyzer (resolution: 100 kHz) at two different base stations. The first base station (BS1), which was located at the outskirts of a large city, had a traffic intensity of  $\sim 7$  Erlangs. The second base station (BS2) placed at downtown had a traffic intensity of  $\sim 16$  Erlangs. Fig. 3 shows that the received signal power varied about 11 dB at BS1 and 15 dB at BS2 (99% of time). The average received power of the upstream CDMA signal is proportional to the number of active users [12]. Thus, if we accept the blocking probability of 1%, the power variation of the upstream CDMA signals would be 18 dB for the maximum traffic intensity of 30 Erlangs. By adding 10 dB headroom for the system margin, we obtained that the required upstream dynamic range should be 28 dB, which can be translated to the

<sup>1</sup>See the Qualcomm home page: <http://www.qualcomm.com>.

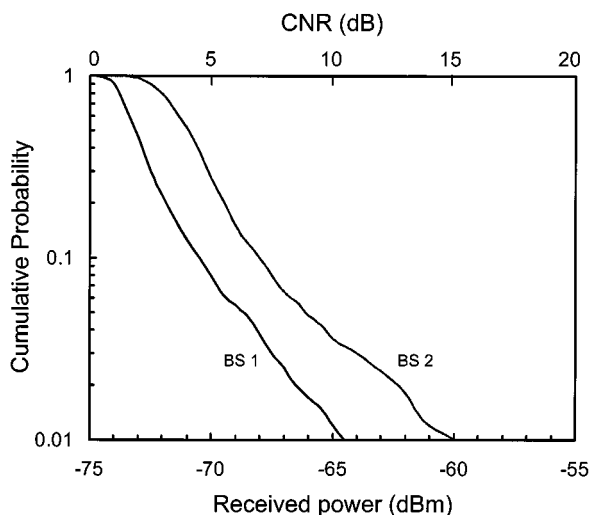


Fig. 3. Dynamic range of upstream CDMA signals measured at commercial PCS base stations. The first base station (BS1), which was located at the outskirts of a large city, had a traffic intensity of  $\sim 7$  Erlangs. The second base station (BS2) placed at downtown had a traffic intensity of  $\sim 16$  Erlangs.

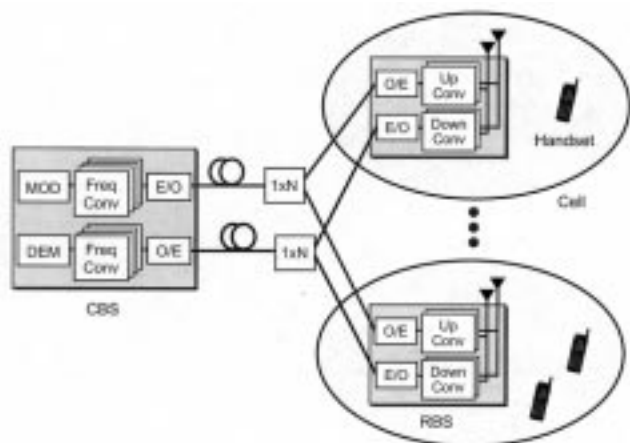


Fig. 4. Schematic diagram of the proposed PON for CDMA-based micro-cellular communication systems.

SFDR of  $68 \text{ dB/Hz}^{2/3}$  (since the noise bandwidth of CDMA signal is 1.23 MHz). The measured dynamic range of the CDMA signal was similar to the value ( $\sim 30 \text{ dB}$ ) reported in other literature [12], [13]. This relaxed requirement is due to the stringent power control ( $\sim 80 \text{ dB}$ ) included in the CDMA mobile transceivers. Thus, unlike the TDMA-based systems (which requires  $>60 \text{ dB}$  of dynamic range), the fiber-optic network for CDMA-based wireless communication system could be implemented by using low-cost optical sources for the upstream traffic. For example, the uncooled, unisolated FP and DFB lasers have been used for the transport of upstream CDMA signals over 18-km-long single-mode fiber (SMF) [12]. The relaxed dynamic range requirement of CDMA signals would also allow the use of various network configurations such as passive double-star, bus, and hybrid fiber-coax (HFC) [13]–[16]. Fig. 4 shows the schematic diagram of passive double-star network for CDMA PCS. In this network, each RBS is accessed by using intermediate frequencies (IFs).

Although this architecture requires up/down converters at each RBS, it offers many advantages. For example, it requires only one optical source for the signals transmitted to each RBS, provides optical fiber gain, and mitigates frequency requirements of various optical and electrical components. The optical beat interference (OBI) caused by optical sources at multiple RBSs could be suppressed by using either the wavelength-selected DFB lasers or broad-band optical sources such as LEDs [17].

#### A. PON with Double-Star Architecture

We first analyzed the performance of a PON with  $M$  RBSs. The performance of this network would be limited by the upstream transmission. Thus, we evaluated the upstream performance by using the carrier-to-noise-and-distortion ratio (CNDNR) at the receiver, which can be described as

$$\text{CNDNR}^{-1} = \text{CNR}_{\text{RX}}^{-1} + \text{CNR}_{\text{sh}}^{-1} + \text{CNR}_{\text{RIN}}^{-1} + \text{CNR}_{\text{OBI}}^{-1} + \text{CDR}_{\text{CTB}}^{-1} + \text{CDR}_{\text{cl}}^{-1}. \quad (1)$$

The first three terms on the right of this equation represent the CNRs by receiver noise, shot noise, and RIN, respectively. These three terms can be written as

$$\text{CNR}_{\text{RX}} = \frac{m^2 I_0^2}{2B \langle i_{\text{RX}}^2 \rangle} \quad (2)$$

$$\text{CNR}_{\text{sh}} = \frac{m^2 I_0}{4qBM} \quad (3)$$

$$\text{CNR}_{\text{RIN}} = \frac{m^2}{2\text{RIN} \cdot BM} \quad (4)$$

where

- $m$  optical modulation index (OMI);
- $I_0$  photocurrent from the signal source;
- $\langle i_{\text{RX}}^2 \rangle$  thermal noise of the receiver;
- $B$  noise bandwidth;
- $q$  electrical charge;
- RIN relative intensity noise of the optical sources.

In these equations, we assumed that the upstream optical source at each RBS emitted the same optical power.

The fourth term on the right of (1) represents the CNR degradation due to OBI. In a PON, the upstream light sources placed at RBSs could generate the OBI noise at the receiver and degrade the system's performance. To characterize the effect of OBI noise, it is helpful to utilize the relative optical beat interference noise (ROBIN) [18]. ROBIN is analogous to the definition of RIN and represents the amount of wavelength overlap between two interfering signals. Thus, the carrier-to-OBI-noise ratio can be expressed as

$$\text{CNR}_{\text{OBI}} = \frac{m^2}{2B \sum_{i,j,i \neq j}^M \text{ROBIN}_{ij}} \quad (5)$$

where  $\text{ROBIN}_{ij}$  represents ROBIN between optical sources at RBS  $i$  and RBS  $j$  [18]. It should be noted that the OBI noise is determined by the convolution of the optical power spectral densities of two interfering optical signals. Thus, ROBIN is very

sensitive to the spectral shape of the optical sources. For example, when DFB lasers (with Lorentzian line shape) were used for upstream optical sources, ROBIN is given by

$$\text{ROBIN}_{ij} = \frac{4}{\pi} \frac{\Delta\nu_F}{\Delta\nu_F^2 + \delta\nu_{ij}^2} \quad (6)$$

where  $\Delta\nu_F$  is the linewidth of the optical source and  $\delta\nu_{ij}$  is the difference between the center optical frequencies of the two interfering optical sources  $i$  and  $j$  [19]. Thus, when the upstream DFB lasers had linewidth of 10 MHz and the optical frequencies of these lasers were separated by more than 0.3 nm ( $\sim 40$  GHz), ROBIN would become as low as  $-140$  dB/Hz. Equation (5) shows that the carrier-to-OBI-noise ratio decreases linearly as the number of RBSs increases if the DFB lasers had equal channel spacing. On the other hand, the ROBIN for the broad-band optical sources such as LEDs can be described as

$$\text{ROBIN} = \frac{1}{\pi} \frac{4}{\Delta\nu_F}. \quad (7)$$

The ROBIN generated from LEDs is independent of the wavelength separation,  $\delta\nu$ , due to their broad spectra. For typical LEDs (linewidth = 50 nm at 1.3  $\mu\text{m}$ ), ROBIN is about  $-128$  dB/Hz. However, the  $\text{CNR}_{\text{OBI}}$  decreases rapidly as the number of LEDs (i.e., RBSs) increases. This is because, in a PON with  $M$  RBSs, there are  $M^2$  combinations of ROBIN generated in pairs and the  $\text{CNR}_{\text{OBI}}$  is degraded by a factor of  $M(M-1)/2$ . Nevertheless, LEDs could be more attractive than DFB lasers for the use in the PON. In case of using the DFB lasers at RBSs, ROBIN could be as high as  $-70$  dB/Hz if the optical spectra of any two lasers accidentally overlapped each other. Thus, to avoid the OBI-induced impairment, it is essential to operate every DFB lasers at different wavelengths (at least several tens of gigahertz away from each other) [20]. This would require the use of wavelength-selected DFB lasers with wavelength-stabilization circuit at every RBS, which would increase the cost of RBSs significantly.

The fifth term on the right of (1) represents the carrier-to-distortion ratio (CDR), which can be written as [2]

$$\text{CDR}_{\text{CTB}} = \frac{\text{IP}_3^2}{4N_{\text{IM3}}P_{\text{in}}^2} \quad (8)$$

where

- $N_{\text{IM3}}$  number of third-order intermodulation tones;
- $P_{\text{in}}$  input RF power;
- $\text{IP}_3$  input third-order intercept point.

In this equation, we ignored the second-order intermodulation term since most fiber-optic networks for transporting wireless signals utilize less than one octave of bandwidth. Thus, for  $N$  carriers, the number of intermodulation tones at the  $k$ th subcarrier can be described as

$$N_{\text{IM3}} = \frac{k}{2}(N-k+1) + \frac{1}{4}\{(N-3)^2 - 5\} - \frac{1}{8}\{1 - (-1)^N\}(-1)^{N+k} \quad (9)$$

where  $k = 1$  represents the first channel [2]. The highest number of intermodulation terms, which falls on the center of the signal band, becomes to be  $(3N^2 - 14N + 8)/8$ .

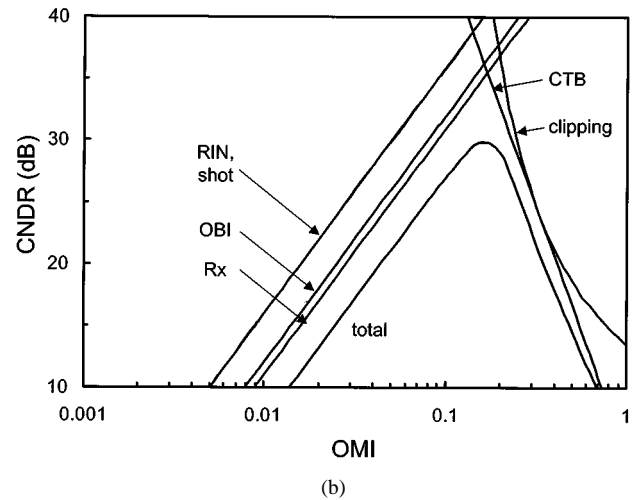
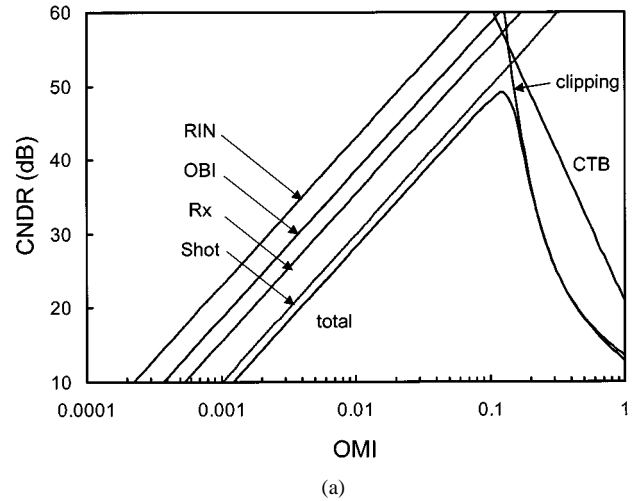


Fig. 5. CNDR versus OMI for various noise and distortion terms for upstream transmission. (a) Wavelength-selected DFB lasers (b) Light-emitting diodes. The device parameters used in this figure are listed in Table I.

The last term on the right of (1) represents the CDR degradation due to clipping distortion, which occurs when the bias current falls below threshold current instantaneously [21]. It can be expressed as

$$\text{CDR}_{cl} = \frac{\sqrt{2\pi}(1 + 6\mu^2)}{\mu^3} \exp\left(\frac{1}{2\mu^2}\right) \quad (10)$$

where  $\mu$  is the total rms modulation index ( $m(N/2)^{1/2}$ ). The clipping distortion becomes important when the total rms modulation index is greater than  $\sim 25\%$ .

Fig. 5(a) and (b) shows the CNDR limited by various noise and distortion terms for the cases of using DFB lasers and LEDs for upstream transmission, respectively. In these figures, we assumed that eight RBSs were connected to the CBS via  $1 \times 8$  star coupler and the link loss was 15 dB [9 dB (star coupler) + 3 dB (fiber) + 3 dB (WDM or directional coupler)]. The other parameters are summarized in Table I. As shown in Fig. 5(a), when we used DFB lasers with wavelength separation of 0.8 nm, the OBI noise was much smaller than the shot noise. Thus, the performance of this system would be limited by the shot noise when the OMI was set to be within 8%. However, the clipping distortion became dominant as the OMI increased to  $> 10\%$ .

TABLE I  
OPTICAL DEVICE PARAMETERS USED IN FIG. 5

Devices	Symbol	Description	Values
DFB laser	$P_o$	Output power	1 mW
	$RIN$	Relative intensity noise	-155 dB/Hz
	$IP_3$	3-rd order intercept point	20 dBm
	$\eta$	slope efficiency	0.15 W/A
LED	$P_o$	Output power	0.1 mW
	$\Delta\nu_F$	Linewidth	50 nm
	$IP_3$	3-rd order intercept point	25 dBm
	$\eta$	slope efficiency	2.5 mW/A
Receiver	$\langle i_{RX} \rangle$	Receiver noise current	4 pA/ $\sqrt{\text{Hz}}$
	$\rho$	Responsivity	0.9 A/W

Fig. 5(b) shows the performance of upstream transmission when we used low-cost LEDs instead of the wavelength-selected DFB lasers. In this case, the maximum achievable dynamic range was limited to about 30 dB. Both the OBI and receiver noises contributed to this limitation almost equally, if the OMI was set to be smaller than 20%. However, when the OMI exceeded 20%, spurious components generated by the nonlinear characteristic of LED became dominant over the clipping distortion.

### B. Experiments

Fig. 6 shows the experimental setup to demonstrate the passive double-star network for wireless CDMA services depicted in Fig. 4. We have implemented the proposed network with various optical sources (such as DFB lasers, FP lasers, and LEDs) to examine the possibility of using inexpensive components. The experimental setup for the downstream is shown in Fig. 6(a). We have used either a 1.55- $\mu\text{m}$  DFB laser or a 1.3- $\mu\text{m}$  FP laser. The output powers of the DFB laser and FP laser were 1.7 mW and 0.7 mW, respectively. The CBS transmitted 32 CDMA signals to eight RBSs (i.e., four CDMA signals to each RBS) and these signals were down-converted to the IF region of 247–433 MHz. In general, each CDMA signal (bandwidth: 1.23 MHz) can support about 30 voice channels [22]. We used one CDMA signal and 31 tone-signals spaced at 6 MHz. The CDMA signal was down-converted from 1.81 GHz to 337 MHz and placed at the center of the IF region to measure the signal degradation by the spurious components. The downstream signals traversed through 10 km of SMF to a 1  $\times$  8 optical splitter. The total link loss was 16 dB at 1.3  $\mu\text{m}$  and 13.5 dB at 1.55  $\mu\text{m}$ . A PIN-FET receiver was used at each RBS. The performance of the downstream transmission was evaluated by measuring the CNR and waveform quality by using an RF spectrum analyzer and a CDMA cell site test set, respectively.

Fig. 6(b) shows the experimental setup for the upstream transmission. We assumed that each RBS utilized two independent antennas for spatial diversity to avoid signal degradation due to the multiple reflection of radio signals. Thus, each RBS should down-convert eight CDMA signals to IF region and transmit to the CBS. We have first implemented the RBSs by using wavelength-selected DFB lasers. Eight DFB lasers were connected to the 1  $\times$  8 star coupler to simulate the situation with eight

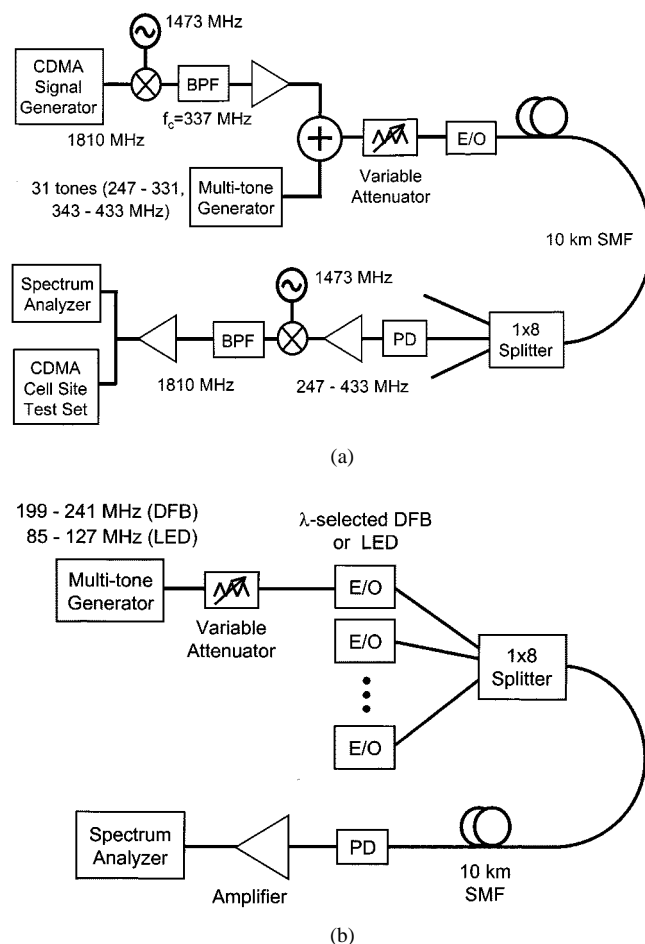


Fig. 6. Experimental setup to demonstrate the proposed PON. (a) Downstream. (b) Upstream.

RBSs. These lasers operated in the spectral region of 1547–1558 nm with the minimum spacing larger than 0.2 nm. We modulated one laser with eight IF tones spaced at 6 MHz between 199 and 241 MHz, while operating seven lasers without modulation. We have also used low-power (70  $\mu\text{W}$ ) LEDs operating at 1.3  $\mu\text{m}$  instead of the wavelength-selected DFB lasers. The spectral width of the LEDs was about 65 nm. In this case, however, the IFs were chosen to be around 100 MHz to avoid the signal degradation by the limited bandwidth of the LEDs.

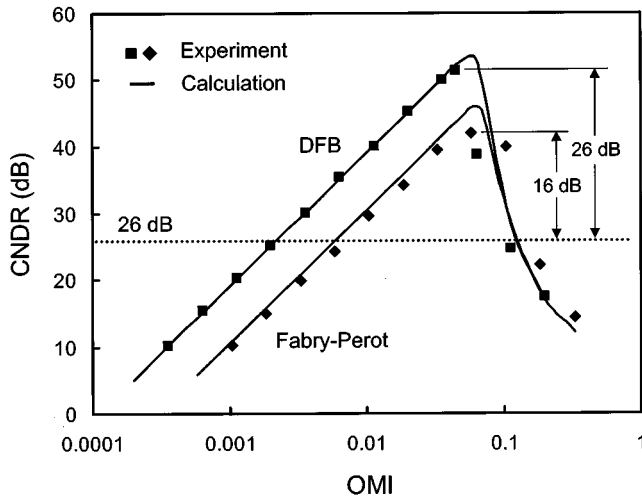


Fig. 7. Measured CNDR versus OMI for the downstream (after 10-km transmission). The CBS transmits 32 CDMA signals to eight RBSs (four CDMA signals for each RBS).

### C. Results

Fig. 7 shows the measured CNDR versus OMI for the downstream in comparison with the calculated curves using (1)–(10). The OMI could not exceed 8% since the CNDR was reduced drastically by the clipping distortion for both types of lasers. When the DFB laser was used to transmit 32 CDMA signals (and the OMI was set to be within 8%), the downstream performance was mainly limited by shot noise. However, when we used an unisolated FP laser, the thermal noise limited the system's performance due to the low output power (0.7 mW) and large fiber loss (16 dB). We did not observe any significant impulse noise caused by Rayleigh backscattering [12], [23]. Typically, an analog fiber-optic link transporting CDMA signals requires a minimum dynamic range of about 26 dB (including 15-dB margin) for the downstream transmission [12]–[14]. The measured results show that both types of lasers could well satisfy this dynamic range requirement of 26 dB.

Fig. 8 shows the measured waveform quality versus OMI. The waveform quality represents the normalized cross-correlation of the transmitted RF waveform in comparison to the ideal waveform. This is an important measure of system's performance since the CDMA signals require correlative receivers. For the downstream, the waveform quality should be better than 0.912 when the CBS transmits the pilot channel only [24]. The results show that the DFB and FP laser have 41- and 32.5-dB margin, respectively, when the spurious components are less than 45 dBc (OMI = 8%). However, it should be noted that these margins are about 15 dB higher than the extra margins shown in Fig. 7 since the waveform quality criterion (0.912) does not include the system margin of 15 dB.

Fig. 9 shows the CNDR versus OMI for the upstream measured by using wavelength-selected DFB lasers and LEDs. The performance of the upstream was mainly limited by the shot noise for wavelength-selected DFB lasers. There was no degradation in CNR due to the OBI since the wavelengths of DFB lasers were separated by at least 0.2 nm. The maximum CNDR was measured to be 52 dB for the wavelength-selected DFB

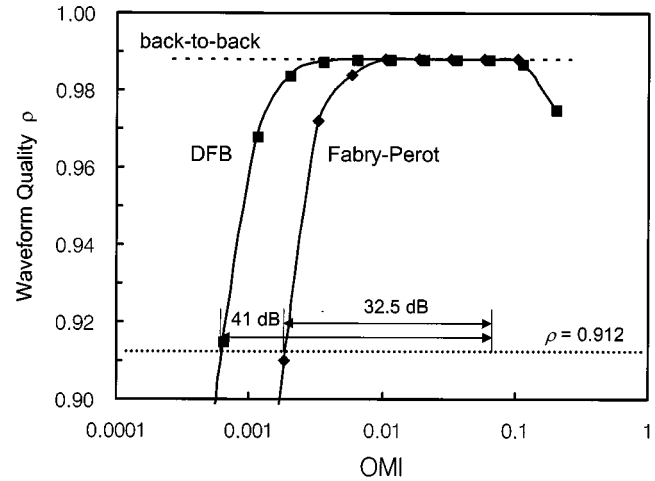


Fig. 8. Measured waveform quality versus OMI for the downstream (after 10-km transmission). The dashed line (back-to-back) was measured as a reference line by connecting the CDMA signal generator to the CDMA cell site test set directly without E/O and O/E conversions.

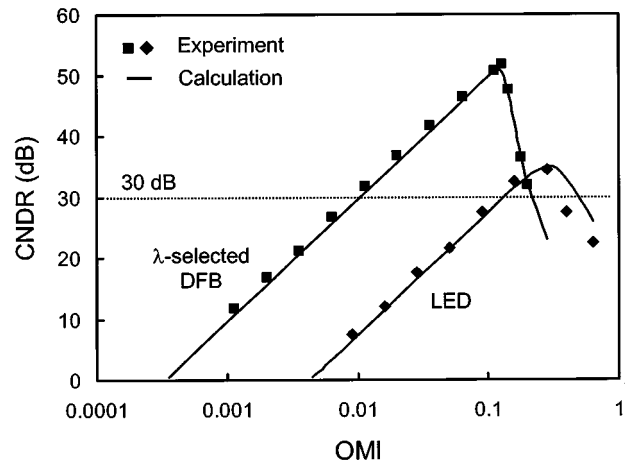


Fig. 9. Measured CNDR versus OMI for the upstream (after 10-km transmission). We assumed that each RBS should transmit eight CDMA signals (instead of four signals) to the CBS to accommodate diversity antenna.

lasers, which satisfied the requirement of the upstream transmission (30 dB). However, when we used LEDs instead of wavelength-selected DFB lasers, the measured CNDR could not exceed 34.5 dB due to the OBI. As shown in (5), this OBI-limited CNR could not be improved easily unless the splitting ratio was reduced. Nevertheless, it should be noted that the low-cost LEDs could still satisfy the dynamic range requirement of 30 dB for the upstream transmission.

These results confirmed that the proposed network could be implemented cost-effectively by using a FP laser and LEDs for downstream and upstream signals, respectively. However, the performance of this network was still limited by the OBI noise of the upstream signals, despite the broad linewidth of LEDs. Thus, the proposed network could accommodate not much more than eight RBSs. Since the OBI noise depends only on the LEDs linewidth, the scalability of this network could not be improved easily even if we increased the output powers of LEDs. This problem could be solved by using wavelength-selected DFB

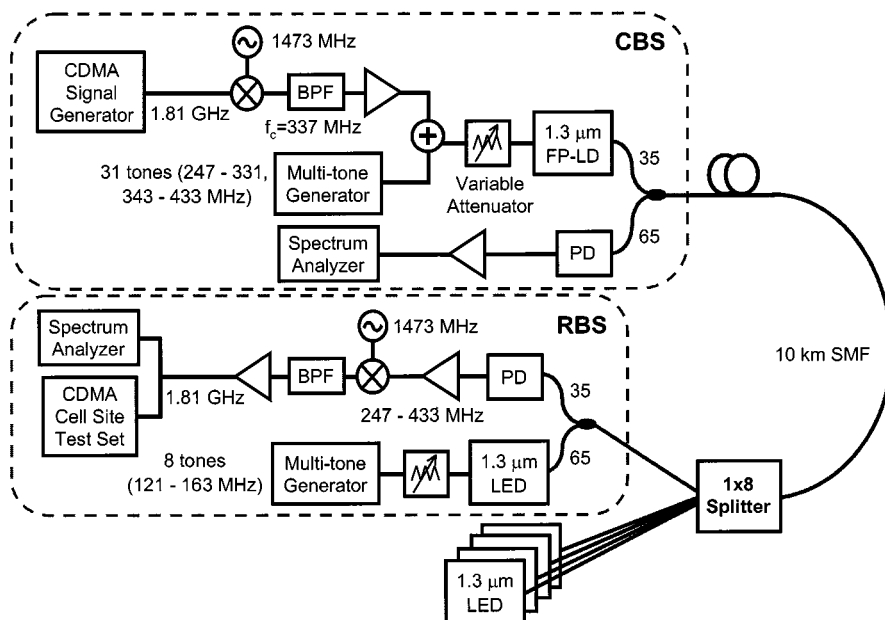


Fig. 10. Experimental setup to demonstrate the proposed bidirectional PON.

lasers at RBSs. However, these lasers would require tight wavelength-stabilization circuits at RBSs, which may not be desirable in practice.

### III. BIDIRECTIONAL PON FOR CDMA-BASED WIRELESS COMMUNICATION SYSTEM

To enhance the cost-effectiveness of the proposed PON, we evaluated the possibility of using bidirectional transmission over single strand of fiber. For the bidirectional transmission, it is necessary to use either SCM or WDM technique to avoid crosstalk between the upstream and downstream signals. In case of using the SCM technique, the bidirectional signals should use two different RF bands since both the downstream and upstream signals operate at the same wavelength. The crosstalk generated by Rayleigh backscattering could be suppressed by using RF filters [25]. On the other hand, the WDM technique utilizes different wavelengths for the upstream and downstream traffics. Thus, it is necessary to use the wavelength-division-multiplexed (WDM) couplers at the end of transmission fiber to separate the bidirectional signals and suppress the crosstalk.

#### A. Bidirectional PON Using SCM Technique

We have first demonstrated the bidirectional PON by using SCM technique. Fig. 10 shows the experimental setup. A 1.3- $\mu\text{m}$  FP laser and 1.3- $\mu\text{m}$  LEDs were used for the upstream and downstream transmission, respectively. The bidirectional transmission was achieved by using different RF bands for upstream and downstream signals. The downstream signals used 247–433 MHz band while the upstream signals used relatively low RF band of 127–163 MHz due to the inherently narrow modulation bandwidth of LEDs. As in the previous experiment, we used one CDMA signal and 31 tones spaced at 6 MHz for downstream transmission. The CDMA signal was down-converted from 1.81 GHz to 337 MHz so that it can be

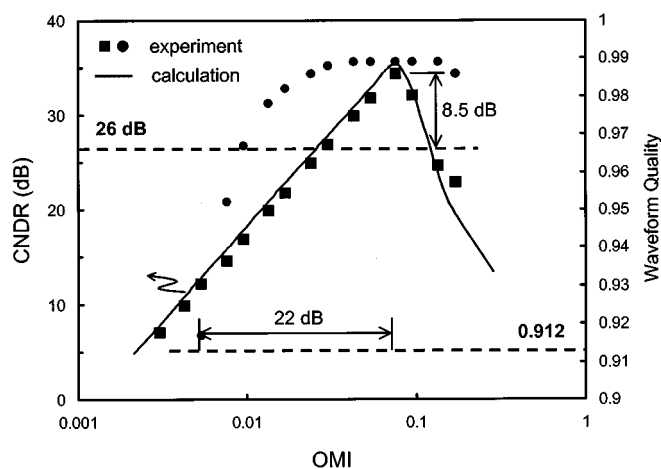


Fig. 11. Measured CNDR and waveform quality of the bidirectional PON using SCM technique for downstream transmission.

placed at the center of the IF region. The output power of the FP laser was 0.2 dBm. After 10-km transmission, the received power was measured to be  $-23$  dBm. For the upstream, we used 1.3- $\mu\text{m}$  LEDs to suppress the OBI caused by multiple optical sources at RBSs. The output powers and spectral width of these LEDs were  $-10$  dBm and  $\sim 50$  nm, respectively. We used 65:35 couplers at the end of transmission fiber to separate the bidirectional signals. This coupling ratio was used to enhance the upstream performance without sacrificing the downstream performance significantly. The asymmetry of the coupling ratio could be increased further if a high-power laser were used for the downstream transmission.

Fig. 11 shows the measured CNDR and waveform quality as a function of OMI for the downstream. When the OMI was set to be within 8%, the downstream performance was mainly limited by the thermal noise of the receiver. The experimental results confirmed that the FP laser could satisfy both the dynamic

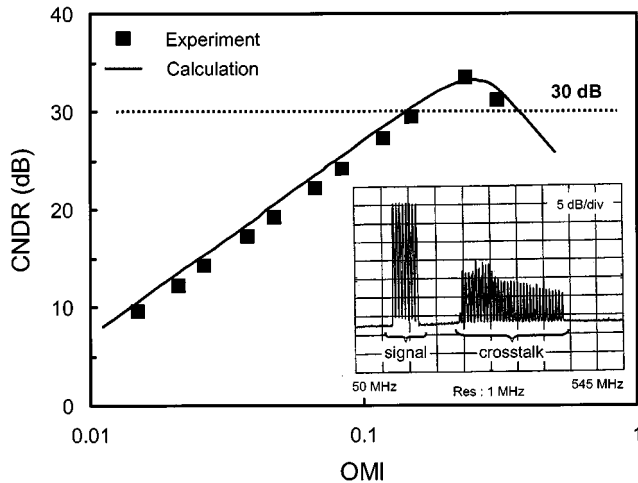


Fig. 12. CNR versus OMI of the bidirectional PON using SCM technique for upstream transmission. The inset shows the upstream spectrum measured at the CBS.

range and waveform quality criterion for the downstream. When an unisolated FP laser and LEDs were used for downstream and upstream traffic, respectively, in a bidirectional SCM system, the system's performance could suffer from the destabilization of the FP laser caused by either Rayleigh backscattering or optical reflection from the upstream LED, depending on the fiber length [26]. The typical back-reflection of commercial LEDs are about  $-10$  dB. However, the Rayleigh backscattering induced reflection of a 10-km-long fiber is merely  $-32$  dB (at  $1.3 \mu\text{m}$ ). Thus, when the fiber length is short ( $< \sim 10$  km), the system's performance is impaired by the optical reflection from the upstream LEDs. Conversely, when the fiber length is long, the Rayleigh backscattered light becomes dominant since the reflected light from the upstream LEDs suffers the link loss twice. In this experiment, however, we did not observe any performance degradation caused by either Rayleigh backscattering or optical reflection. This was because the  $1 \times 8$  coupler increased the link loss significantly and the thermal noise of the receiver became dominant over the sporadic noises (generated by Rayleigh backscattering and/or optical reflection from the upstream LEDs).

Fig. 12 shows the CNDR versus OMI for the upstream. The inset is the upstream spectrum measured at the CBS. We observed significant crosstalk components at the downstream signal band (247–433 MHz) and attributed this to the OBI between the Rayleigh backscattered light (from the FP laser) and upstream LED signals [25]. This was confirmed by measuring the crosstalk level while changing the output power of LEDs. However, these crosstalk components were removed easily by using RF filters and did not deteriorate the upstream performance. In addition, the noise level at the upstream signal band (121–163 MHz) remained unchanged even when we turned off the FP laser to remove the OBI-induced crosstalk completely. These results indicate that the upstream performance was not affected by the bidirectional transmission. Thus, the dominant limiting-factor for the upstream performance would be the OBI generated among multiple LEDs. The maximum CNDR for the upstream was measured to be about 33.5 dB, which satisfied the dynamic range requirement of 30 dB.

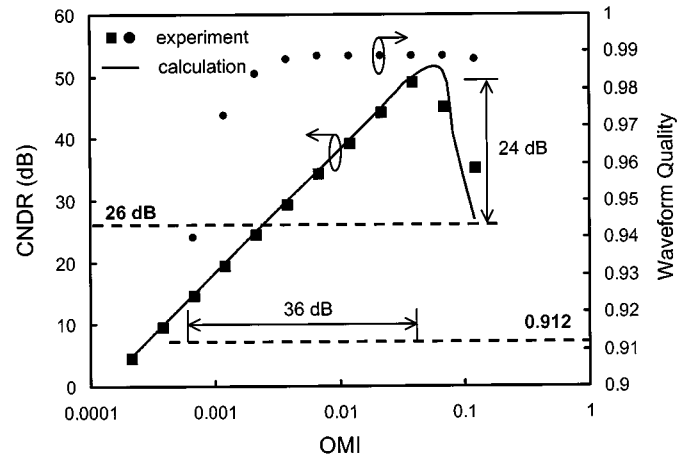


Fig. 13. Measured CNR and waveform quality of the bidirectional PON using WDM technique for downstream transmission.

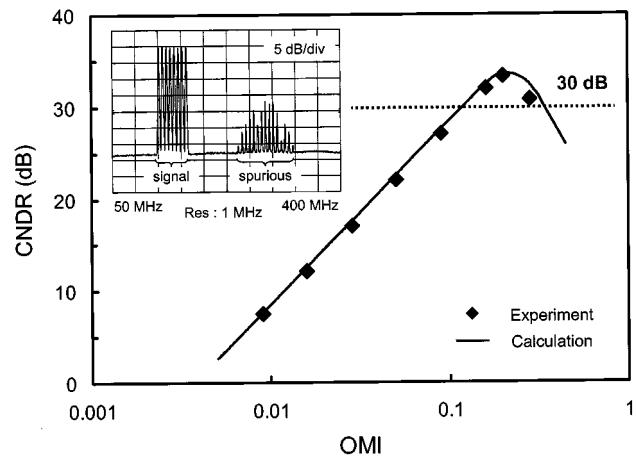


Fig. 14. CNR versus OMI of the bidirectional PON using WDM technique for upstream transmission. The inset shows the upstream spectrum measured at the CBS.

### B. Bidirectional PON Using WDM Technique

The proposed PON could also be implemented by using WDM technique. We demonstrated such a network by replacing the  $1.3\text{-}\mu\text{m}$  FP laser in Fig. 10 with a  $1.55\text{-}\mu\text{m}$  DFB laser. The DFB laser had an output power of 1.7 mW. The upstream optical sources were the same  $1.3\text{-}\mu\text{m}$  LEDs. The 65:35 couplers, placed at the end of transmission fiber, were also replaced with WDM couplers. Due to the high optical isolation of these couplers ( $> 45$  dB), the RF crosstalk was suppressed to be less than  $-90$  dB.

Fig. 13 shows the measured CNDR and waveform quality as a function of OMI for the downstream. Since the link loss of this network (17 dB) was much less than the network using SCM technology (23 dB), the achievable dynamic range was improved to 48 dB. The RF power margin for waveform quality was also increased to 36 dB comparing to the network using SCM technology (22 dB).

Fig. 14 shows the CNDR versus OMI for the upstream. Again, the inset is the upstream spectrum measured at the CBS. In this case, however, the spurious components at 250–

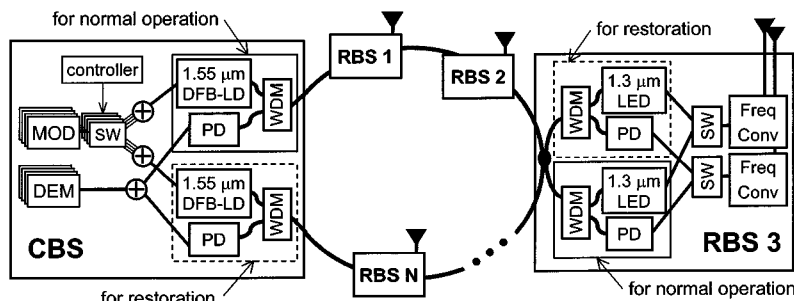


Fig. 15. Schematic diagram of bidirectional SCM self-healing ring network using RF switches for restoration.

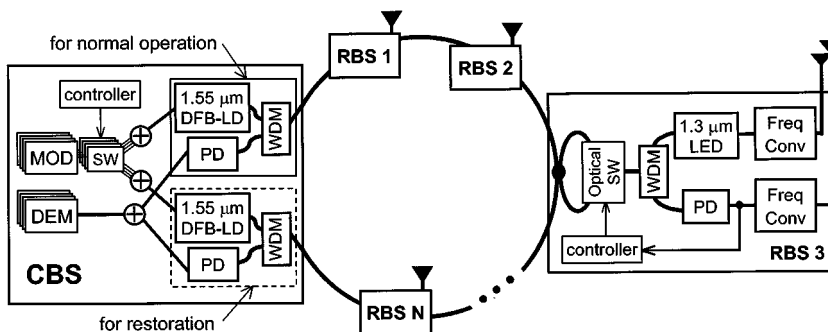


Fig. 16. Schematic diagram of bidirectional SCM self-healing ring network using optical switches for restoration.

320 MHz range were attributed to the second-order nonlinearity of the LEDs. There was no crosstalk originated from the bidirectional transmission due to the high optical isolation of WDM couplers. This bidirectional network also satisfied the dynamic range requirement for the upstream transmission.

#### IV. BIDIRECTIONAL SELF-HEALING RING NETWORK FOR CDMA-BASED WIRELESS COMMUNICATION SYSTEM

The proposed PON based on double-star architecture provides fiber gain and reduces the number of optical sources for downstream transmission. However, in this network, an accidental fiber-cut between the CBS and splitter could disrupt communications for  $\sim 1000$  subscribers ( $\approx 30$  subscribers/channel  $\times 4$  channels/RBS  $\times 8$  RBSs). This problem of reliability could be resolved by modifying the proposed network to have ring architecture. For example, Fig. 15 shows a bidirectional self-healing ring network for CDMA-based wireless services. In this network, each base station is equipped with two transceivers: one for normal operation and the other for restoration. In normal operation, the CBS transmits downstream signals in the clockwise direction while RBSs transmit upstream signals in the counterclockwise direction. However, in case of fiber cut, the control circuits at the CBS and RBSs detect the transmission failure by monitoring the received RF signals and then trigger the relevant RF switches to transfer the RF signals to the other transceiver. For example, when a fiber cut occurs between RBS 1 and RBS 2, the CBS transmits the downstream signals for RBS 2  $\sim$  RBS N in the counterclockwise direction (using the transmitter for restoration) while the downstream signal for RBS 1 is still

transmitted in the clockwise direction (using the transmitter for normal operation). Thus, this network is capable of restoring the fiber failure automatically. In addition, this network is robust to the equipment failure since each RBS is equipped with two transceivers. The restoration time of this network was measured to be less than  $50 \mu s$  for 9.3-km ring since we used fast RF switches (switching time:  $\sim 1$  ns) [27]. The same network could also be implemented by using optical switches as shown in Fig. 16. This network would not require the duplicate transceivers, but have longer restoration time since most commercial optical switches (such as thermo-optical switches and mechanical switches) operate at  $\sim 1$  ms.

In CDMA systems, a pilot channel [composed of repetitive pseudonoise (PN) sequence] is sent from the base station to the mobile transceivers for both the clock recovery and the identification of the base station that they should communicate with. The mobile transceivers identify the base station using the distinct PN offset (i.e, chip delay) since every base station transmits the pilot channels with identical bit patterns (all zero patterns) [28]. Thus, it is specified in IS-95 that the timing of the pilot channel (at the output of base station) should be maintained within  $\pm 3 \mu s$  [24]. In the present CDMA system, this specification is conformed by using the Global Positioning System (GPS) signal received at the base station [28]. However, in a micro-cellular system, it may not be practical to install the GPS receivers at numerous RBSs. Thus, when the fiber-cut is detected, the CBS should adjust the PN offset for each RBS to compensate for the changes in the fiber delay caused by the restoration. With this restoration procedure, the accidental fiber-cut in the proposed ring network would not cause more than a single bit error since the restoration time ( $50 \mu s$ ) is shorter than the bit duration ( $104.2 \mu s$ ) of the CDMA signal.

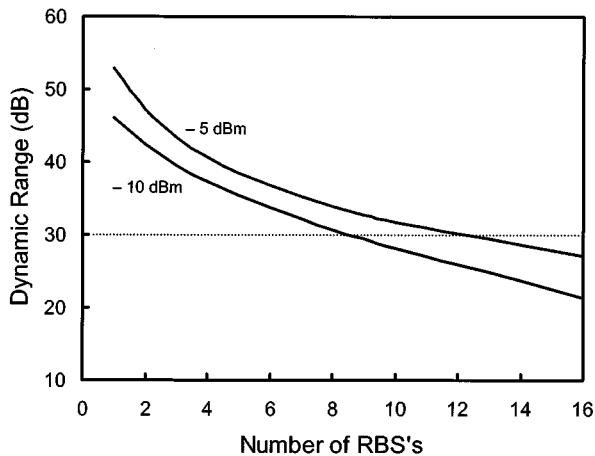


Fig. 17. The scalability of the proposed bidirectional SCM self-healing ring network. For the scalability estimation, we calculated the achievable dynamic range of the upstream signal for the worst RBS.

Fig. 17 shows the scalability of the proposed self-healing ring network. In this network, the downstream performance could be improved easily by increasing the output power of the DFB lasers. Thus, for the scalability estimation, we calculated the achievable dynamic range of the upstream signal for the worst RBS. We assumed that  $N$  RBSs were uniformly distributed in the 10-km ring via 10:1 directional couplers. Thus, the fiber length between each RBS was  $10/(N+1)$  km. The other parameters used in this calculation were as follows: fiber loss = 0.4 dB/km (at 1.3  $\mu\text{m}$ ), insertion loss of WDM coupler = 1.0 dB, excess loss of 10:1 coupler = 0.2 dB, linewidth of LED = 50 nm, and thermal noise of receiver = 3.0 pA/Hz<sup>1/2</sup>. The calculated results show that the proposed network could accommodate up to eight RBSs if we assumed that every LED had an identical optical power of -10 dBm. This scalability could be improved by using high-power LEDs since it was mainly limited by the thermal noise of the receiver. For example, the proposed network should be able to accommodate up to 12 RBSs by increasing the output powers of LEDs to -5 dBm. However, the network's scalability could not be improved further (even if output powers of LEDs were increased higher than -5 dBm) as the OBI noise became dominant over the receiver noise.

## V. SUMMARY

We proposed and demonstrated PONs for CDMA-based microcellular communication systems. The relaxed dynamic range requirements of CDMA signals ( $\sim 30$  dB) allowed us to use various network architectures including double-star, bus, and ring. We have first demonstrated the PON based on double-star architecture. This network has the following advantages.

- 1) It provides optical fiber gain.
- 2) It needs only one optical source for downstream signals.
- 3) It relaxes the frequency requirements of optical and electrical components.

In addition, this network could be implemented by using low-cost LEDs instead of wavelength-selected DFB lasers for upstream signals. The broad linewidth of LEDs suppressed the OBI noise to an acceptable level. To further enhance the

cost-effectiveness of the proposed network, we have also demonstrated a bidirectional PON. There was no significant differences in the performances between the unidirectional and bidirectional PONs. This was because the upstream performances of these networks were limited by the OBI noise, and the increased link losses (due to the couplers) in the bidirectional PON had only a minor effect. We have also demonstrated the proposed network with ring architecture for the self-healing capability. This network could be restored from a fiber or equipment failure within 50  $\mu\text{s}$ . Both the networks using double-star and ring architectures could accommodate about eight RBSs within the network. We believe that these networks could help the development of efficient fiber-optic networks for CDMA-based wireless communication systems.

## ACKNOWLEDGMENT

The authors would like to thank J. M. Cheong of SK Telecom for measuring the dynamic range of upstream CDMA signals at commercial PCS base stations.

## REFERENCES

- [1] T. S. Chu and M. J. Gans, "Fiber optic microcellular radio," *IEEE Trans. Veh. Technol.*, vol. 40, no. 3, pp. 599–606, 1991.
- [2] J. Namiki, M. Shibutani, W. Domon, T. Kanai, and K. Emura, "Optical feeder basic system design for microcellular mobile radio," *IEICE Trans. Commun.*, vol. E76-B, no. 9, pp. 1069–1077, Sept. 1993.
- [3] W. I. Way, "Optical fiber-based microcellular systems: An overview," *IEICE Trans. Commun.*, vol. E76-B, no. 9, pp. 1091–1102, Sept. 1993.
- [4] S. Ariyavistakul, T. E. Darcie, L. J. Greenstein, M. R. Phillips, and N. K. Shankaranarayanan, "Performance of simulcast wireless techniques for personal communication systems," *IEEE J. Select. Areas Commun.*, vol. 14, pp. 632–643, May 1996.
- [5] O. K. Tonguz and H. Jung, "Personal communications access networks usiking subcarrier multiplexed optical links," *J. Lightwave Technol.*, vol. 14, pp. 1400–1409, June 1996.
- [6] Y. Aburakawa and H. Ohtsuka, "Signal extraction with frequency arrangement (SEFA) and superimposed subcarrier modulation (SSM) schemes in fiber-oriented wireless access systems," *J. Lightwave Technol.*, vol. 15, pp. 2223–2231, Dec. 1997.
- [7] K. Emura, "Enabling technologies for SCM based optically fed wireless communication systems," *Opt. Quantum Electron.*, vol. 30, pp. 1089–1101, 1998.
- [8] R. Kohno and M. Nakagawa, "International cooperative research and development of wireless personal communications in Asia-Pacific countries," *IEEE Personal Commun.*, vol. 4, pp. 6–12, Apr. 1997.
- [9] W. I. Way, *Broadband Hybrid Fiber/Coax Access System Technologies*. New York: Academic, 1999, ch. 10.
- [10] D. M. Cutrer, J. B. Georges, T. H. Le, and K. Y. Lau, "Dynamic range requirements for optical transmitters in fiber-fed microcellular networks," *IEEE Photon. Technol. Lett.*, vol. 7, pp. 564–566, May 1995.
- [11] J. C. Fan, C. L. Lu, and L. G. Kazovsky, "Dynamic range requirements for microcellular personal communication systems using analog fiber-optic links," *IEEE Trans. Microwave Theory Tech.*, vol. 45, pp. 1390–1397, Aug. 1997.
- [12] S. L. Woodward and S. Ariyavistakul, "Transporting CDMA signals over an analog optical link," *IEEE Trans. Veh. Technol.*, vol. 48, pp. 1033–1038, July 1999.
- [13] H. Kim, J. M. Cheong, C.-H. Lee, and Y. C. Chung, "Passive optical network for microcellular CDMA personal communication service," *IEEE Photon. Technol. Lett.*, vol. 10, pp. 1641–1643, Nov. 1998.
- [14] H. Kim and Y. C. Chung, "Bi-directional passive optical network for CDMA personal communication service," *Electron. Lett.*, vol. 35, no. 4, pp. 315–317, Feb. 1999.
- [15] J. M. Cheong, S. H. Seo, Y. S. Son, T. G. Kim, H. Kim, Y. C. Chung, and S. Park, "Field trial experiment of CDMA fiber-optic microcellular system: FoMiCell," in *Proc. OFC Conf.*, San Diego, CA, Feb. 1999, paper PD13.

- [16] Y. M. Lin and W. I. Way, "The feasibility study of transporting IS-95 CDMA signals over HFC networks," *IEEE Photon. Technol. Lett.*, vol. 11, pp. 736–738, June 1999.
- [17] R. D. Feldman, K.-Y. Liou, G. Raybon, and R. F. Austin, "Reduction of optical beat interference in a subcarrier multiple-access passive optical network through the use of an amplified light-emitting diode," *IEEE Photon. Technol. Lett.*, vol. 8, pp. 116–118, Jan. 1996.
- [18] S. L. Woodward, J. W. Stayt, D. M. Romero, J. M. Freund, and G. J. Przybylek, "A study of optical beat interference between Fabry-Perot lasers," *IEEE Photon. Technol. Lett.*, vol. 10, pp. 731–733, May 1998.
- [19] D. J. G. Mestdagh, *Fundamentals of Multiaccess Optical Fiber Networks*. Norwood, MA: Artech House, 1995, ch. 8.
- [20] T. H. Wood and N. K. Shankaranarayanan, "Operation of a passive optical network with subcarrier multiplexing in the presence of optical beat interference," *J. Lightwave Technol.*, vol. 11, pp. 1632–1640, Oct. 1993.
- [21] T. E. Darcie, "Subcarrier multiplexing for lightwave networks and video distribution systems," *IEEE J. Select. Areas Commun.*, vol. 8, pp. 1240–1248, Sept. 1990.
- [22] R. L. Peterson, R. E. Ziemer, and D. E. Borth, *Introduction to Spread Spectrum Communication*. Englewood Cliffs, NJ: Prentice-Hall, 1995.
- [23] K. D. LaViolette, "The impact of Rayleigh backscatter induced noise on QPSK transmission with Fabry-Perot lasers," *IEEE Photon. Technol. Lett.*, vol. 8, pp. 706–708, May 1996.
- [24] *Mobile Statio-Base Station Compatibility Standard for Dual-Mode Wideband Spread Spectrum Cellular System*, TIA/EIA/IS-95, PN-3422, 1994.
- [25] S. L. Woodward, X. Lu, and A. H. Gnauck, "Bidirectional, subcarrier-multiplexed transmission using 1.3- $\mu$ m Fabry-Perot lasers," *IEEE Photon. Technol. Lett.*, vol. 9, pp. 1409–1411, Oct. 1997.
- [26] H. Kim and Y. C. Chung, "Bidirectional subcarrier-multiplexed transmission system using unisolated optical sources," *IEEE Photon. Technol. Lett.*, vol. 11, pp. 1488–1490, Nov. 1999.
- [27] ———, "Bidirectional subcarrier-multiplexed self-healing ring network for CDMA personal communication service," *Electron. Lett.*, vol. 35, no. 25, pp. 2215–2216, Dec. 1999.
- [28] V. K. Garg, K. Smolik, and J. E. Wilkes, *Applications of CDMA in Wireless/Personal Communications*. Englewood Cliffs, NJ: Prentice-Hall, 1997, ch. 5.

**H. Kim** (S'97–A'01) was born in Seoul, Korea, on May 28, 1972. He received the M.S. and Ph.D. degrees in electrical engineering from the Korea Advanced Institute of Science and Technology (KAIST), Taejeon, Korea, in 1996 and 2000, respectively.

Since September 2000, he has been a Postdoctoral Fellow at KAIST. His research interests include fiber-optic wireless communication systems, fiber nonlinearities, WDM transmission systems, and optical communication systems.

**Y. C. Chung** (S'81–M'83) is a Professor of electrical engineering at the Korea Advanced Institute of Science and Technology (KAIST), Taejeon, Korea, which he joined in 1994. From 1985 to 1987, he was with Los Alamos National Laboratory under the AWU-DOE graduate fellowship program. From 1987 to 1994, he was with the Lightwave Systems Research Department, AT&T Bell Laboratories. His current activities include high-capacity WDM transmission systems, all-optical networks, WDM monitoring techniques, WDM PON, and fiber-optic networks for wireless communications. He has published more than 200 journal and conference papers in these areas and has more than 40 patents issued or pending.